

A Highly Stretchable Liquid Metal Polymer as Reversible Transitional Insulator and Conductor

Hongzhang Wang, Youyou Yao, Zhizhu He, Wei Rao, Liang Hu, Sen Chen, Ju Lin, Jianye Gao, Pengju Zhang, Xuyang Sun, Xiangjiang Wang, Yuntao Cui, Qian Wang, Shijin Dong, Guozhen Chen, and Jing Liu*

Materials with a temperature-controlled reversible electrical transition between insulator and conductor are attracting huge attention due to their promising applications in many fields. However, most of them are intrinsically rigid and require complicated fabrication processes. Here, a highly stretchable (680% strain) liquid metal polymer composite as a reversible transitional insulator and conductor (TIC), which is accompanied with huge resistivity changes (more than 4×10^9 times) reversibly through a tuning temperature in a few seconds is introduced. When frozen, the insulated TIC becomes conductive and recovers after warming. Both the phase change of the liquid metal droplets and the rigidity change of the polymer contribute directly to transition between insulator and conductor. A simplified model is established to predict the expansion and connection of liquid metal droplets. Along with high stretchability, straightforward fabrication methods, rapid triggering time, large switching ratio, good repeatability, the TIC offers tremendous possibilities for numerous applications, like stretchable switches, semiconductors, temperature sensors, and resistive random-access memory. Accordingly, a system that can display numbers and letters via converting alternative TIC temperature to a binary signal on a computer is conceived and demonstrated. The present discovery suggests a general strategy for fabricating and stimulating a stretchable transitional insulator and conductor based on liquid metal and allied polymers.

Materials with temperature-controlled reversible electrical transition between insulator and conductor are of great interest to many fields,^[1–3] including smart switches,^[4] sensors,^[5] semiconductors,^[6,7] and resistive random access memories.^[8,9] Typical metal–insulator transitions (MIT) have been observed

in metal oxides,^[10–12] perovskites,^[13,14] and organic films.^[15,16] However, most of these electronic elements are intrinsically rigid and often lack stretchability, which would impede their further applications requiring the adaptability to bending, stretching, and deforming such as those application situations in wearable electronics and skin like electronics.^[17–19] Therefore, endowing the metal–insulator transitions materials with the high elasticity and stretchability promises great potential towards making soft and stretchable electronics. One of the most intriguing strategies as widely applied to achieve this material is the employment of the hybrid composites containing the polymeric substrates and conductive fillers.^[20] Researchers have incorporated different conductive fillers, such as metal particles,^[21–23] carbon nanotubes,^[24,25] graphene^[26] as building components, with polymeric substrates. And again, most of the above conductive fillers are rigid, which unfortunately sacrifices its soft and stretchable properties. Besides, the stimuli to trigger the electrical transition

are mainly mechanical compressing, stretching, twisting other than the contactless stimuli.

Recently, room temperature liquid metal, owning naturally fluidic and metallic properties,^[27] has been identified to be an ideal alternative to rigid conductive fillers for fabricating soft

H. Wang, Y. Yao, Prof. J. Lin, X. Wang, G. Chen, Prof. J. Liu

Department of Biomedical Engineering

School of Medicine

Tsinghua University

Beijing 100084, China

E-mail: jliubme@tsinghua.edu.cn

Prof. Z. He

Department of Vehicle Engineering

College of Engineering

China Agricultural University

Beijing 100083, China

The ORCID identification number(s) for the author(s) of this article can be found under <https://doi.org/10.1002/adma.201901337>.

DOI: 10.1002/adma.201901337

Prof. W. Rao, S. Chen, J. Gao, P. Zhang, Dr. X. Sun, Dr. Y. Cui,

Dr. Q. Wang, Dr. S. Dong, Prof. J. Liu

Beijing Key Lab of Cryobiomedical Engineering and Key Lab

of Cryogenics

Technical Institute of Physics and Chemistry

Chinese Academy of Sciences

Beijing 100190, China

Prof. W. Rao, S. Chen, J. Gao, Prof. J. Liu

School of Future Technology

University of Chinese Academy of Sciences

Beijing 100049, China

Prof. L. Hu

Beijing Advanced Innovation Center for Biomedical Engineering

School of Biological Science and Medical Engineering

Beihang University

Beijing 100083, China

and stretchable polymer composites.^[28–30] In addition, liquid metal plays a crucial role in developing polymer composites with multiple electrical properties including electrically self-healing,^[31,32] pressure-induced conductivity,^[33] high-*k* dielectric,^[34] and mechanical advantages such as mechanically robust,^[35] and tunable rigidity.^[36] Moreover, liquid metal polymer composites possess high dielectric property as an insulator while can be conductive via concentrated pressure due to the rupture of liquid metal droplets, exhibiting tremendously applicable value.^[32] Although promising, the pressure controlled electrical transition is suffering structural damage and thus is irreversible. Besides, the tensile strain to failure of this liquid metal polymer is 135% strain.^[32,33]

Here we firstly introduce a highly stretchable (up to 680% strain) liquid metal polymer composite that is capable of displaying reversible transition between the insulator and the conductor (resistivity span more than 10⁹ times) through temperature regulation alone. TIC is composed of the liquid metal droplets dispersed in the silicone polymer. It acts as insulative under room temperature but becomes conductive after deep freezing (212 K), with resistivity increasing significantly as temperature rises. After 100 times electrical transition cycles of such material, there appears no evident structure damage such as liquid metal (LM) droplets rupture and electrical performance degradation. The working mechanism to trigger electrical transition of TIC is proposed. Further, we built up a simplified model to illustrate the relationship between droplets size and electrical connection. For the more detailed and quantitative study, we elaborate the different factors concerning the capability of temperature-controlled electrical transition, including the viscosity and curing time of the polymer, liquid metal loadings, droplets size and mixing time. Before curing, the polymer with liquid metal dispersed inside can be either directly deformed or printed into various patterns as desired. Taking advantage of its temperature-controlled conductivity of TIC, we conceive a digital screen system that can display different numbers and letters via converting alternative temperature (electricity transition temperature is 212 K) of this material to the binary signal on a computer (“room temperature” to “0”; lower temperature to “1”). The automatically connecting circuit in response to low-temperature change might be promising in future application of exploration in the extreme environment, where it is uninhabited and accompanied with sharp changes in temperature, such as Mars and the Moon. The detailed experimental results are discussed as follows.

Figure 1a shows that the TIC is electrically insulating ($R > 2 \times 10^8 \Omega$) and the light emitting diode (LED) light is off at room temperature. However, it becomes electrically conductive instantly ($R = 0.05 \Omega$) after completely being cooled, lighting up the LED. When subjected to warming by water, TIC returns to an electrical insulator ($R > 2 \times 10^8 \Omega$). Moreover, freezing can make TIC electrically conductive again (Figure 1a; Movie S1, Supporting Information). To further explore the electrical transition behaviors, the resistivity of TIC as a function of temperature is measured by physical property measurement system (PPMS). As shown in Figure 1b, the resistivity value is infinite (out of range) at the initial state and there is a sharp decline ($1.78 \times 10^{-5} \Omega \text{ m}$) by more than 9 orders at 212 K. Applying to heat, it would remain conductive until the

temperature reaches 243 K. Moreover, the transition of this novel material between electrically insulative and conductive is not merely reversible, but also repeatable. Figure 1c shows the 100 cycles resistance change (9 orders) of TIC by adjusting the temperature. Besides, there is no evident structural damage such as liquid metal droplets rupture or electrical performance degradation was observed after freezing and warming for many times (Figure S1, Supporting Information), indicating that the TIC has excellent extreme-low temperature tolerance.

TIC is mainly composed of liquid metal droplets (75.5% Ga, 24.5% In by weight) dispersed in the Pt-catalyzed silicone polymer. The fabrication methods are described in the experimental section. There are many liquid metal droplets that are enclosed with a thin silicone shell in TIC (Figure S2, Supporting Information), which exhibits electrical insulating. To reveal the science behind the reversible insulator–metal transition in response to the temperature change, we design a structure with three liquid metal droplets dispersed in the silicone polymer. Liquid metal droplets shrivel in soft silicone shell at initial state while bulging out from the silicone after freezing (Figure 1d; Movie S2, Supporting Information). When the temperature recovers, the liquid metal contracts to a liquid state, which is enclosed with the shell again. As we know, liquid metal would expand when it solidifies and contract when liquefies. Figure S3 in the Supporting Information shows the expansion and contraction of the liquid metal droplets in TIC after freezing and heating. Especially, TIC becomes rigid and can maintain its shapes after freezing (Figure S4a and Movie S3, Supporting Information). In addition, the storage modulus of TIC increases sharply at 243 K and changes up to 4000 times (Figure S4b, Supporting Information). If the shell is stretchable, they will swell with expansion of liquid metal, preventing the connection of liquid metal. To describe the transition mechanism of TIC, a schematic illustration of mechanism in electrical transition between insulative and conductive of TIC in response to temperature change has been presented (Figure 1e). After frozen, the silica shell becomes extremely thin and rigid, allowing the rigid expanding liquid metal droplets to bulge out from the rigid polymer and connect with each other to form a conductive path. In addition, when the temperature recovers, the liquid metal contracts to a liquid state with reduced volume, and the rigid silica gel returns to elastic and soft state, packaging the liquid metal droplets inside and breaking the conductive path, which leads to an insulative state.

It is noticed that the temperature to trigger the electrical transition is about 212 K, which is far from the phase change temperature of bulk liquid metal. As we know, the solidification temperature of microsize liquid metal depressed largely compared with bulk liquid metal.^[37] Besides, the underlying mechanism of the temperature-induced reversible metal–insulator transition here is the volume change of liquid metal and the stiffness change of silicone polymer induced by glass transition. The stiffness change of the polymer might be caused by the vitrification, which requires the extremely low temperature. Figure 2a shows the vitrification temperature of the polymer is about 244.5 K. Therefore, we attempted to find a polymer with higher T_g to improve the transition temperature. Poly(vinyl chloride) (PVC) ($T_g = 87^\circ\text{C}$) is applied as the matrix to suspend liquid metal. It is difficult to melt PVC by heating

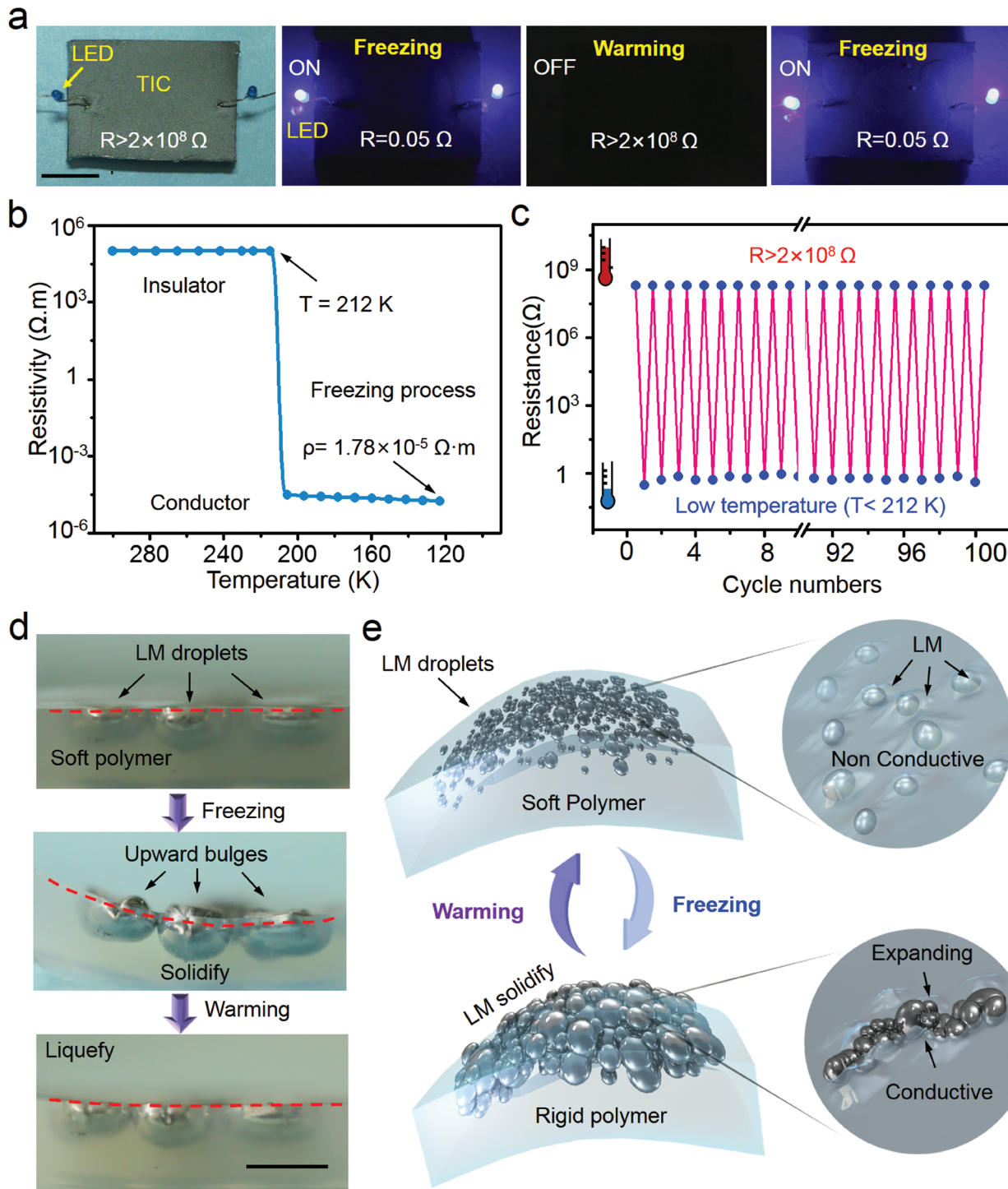


Figure 1. Temperature-induced reversible transitional insulator and conductor (TIC) based on the liquid metal polymer. a) The TIC becomes conductive ($R = 0.05 \Omega$) after freezing by liquid nitrogen and LED is turned on, and recovers to electrical insulative ($R > 2 \times 10^8 \Omega$) again after warming, the scale bar is 2 cm. b) The resistivity of TIC as a function of the temperature. c) Resistance change between electrical insulative and conductive for 100 cycles under the temperature regulation. d) The phase change of LM droplets in response to freezing and warming along with volume change, the scale bar is 2 mm. e) A schematic illustration of mechanism in electrical transition between insulative and conductive of TIC in response to temperature change.

directly. Therefore, we applied dimethyl formamide (DMF) to dissolve the PVC. Liquid metal is fully mixed with liquid PVC and then evaporate the DMF. However, the composite is rigid and lacks stretchability in room temperature. After freezing,

liquid metals are separated from the PVC and deposit at the bottom, which is not conductive (Figure S5, Supporting Information). Hence, PVC composites are not electrically convertible by temperature regulation. The reason of the results is that

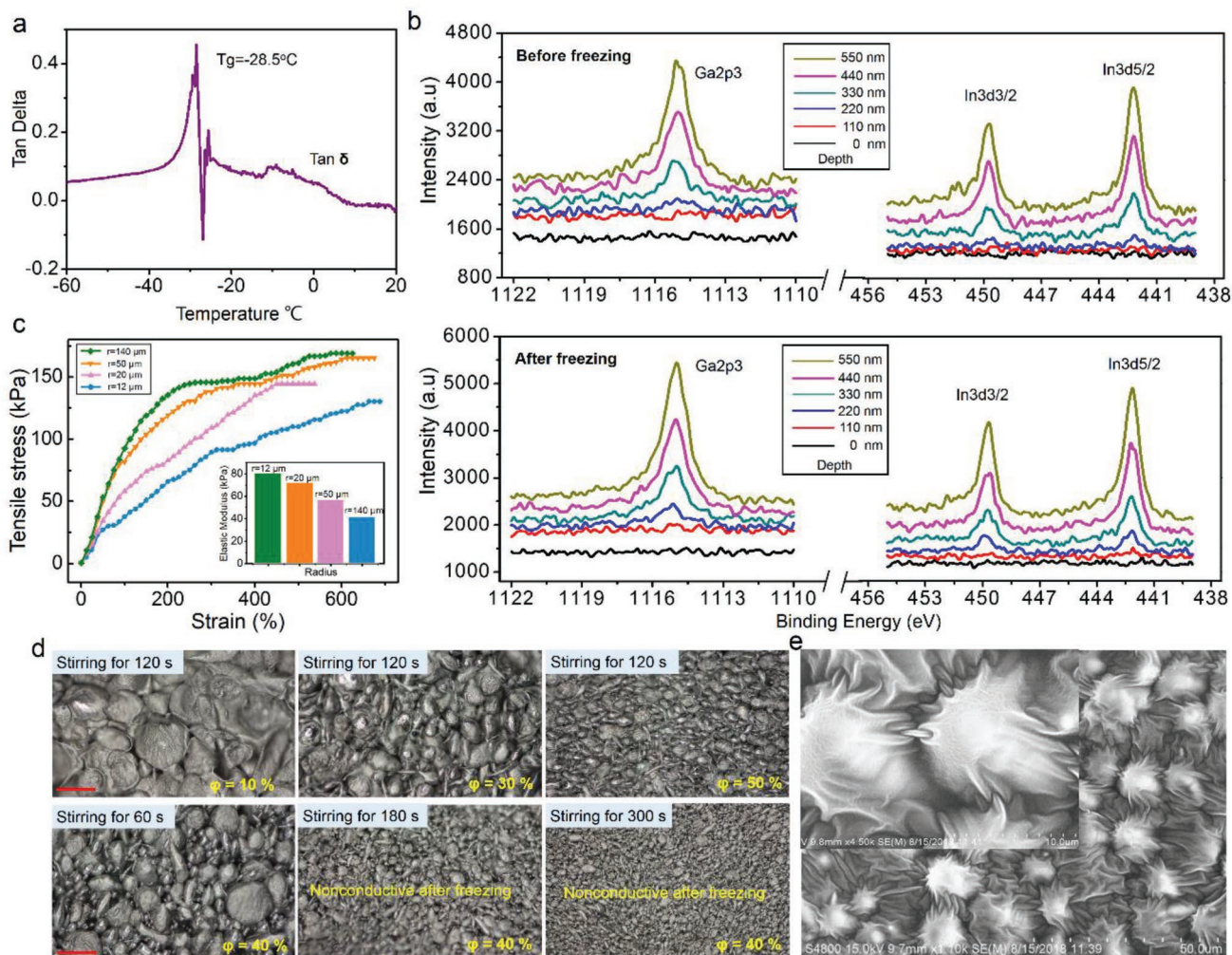


Figure 2. Microstructure analysis of TIC. a) $\tan \delta$ change of TIC as a function of temperature, which shows the glass transition temperature. b) $\text{Ga}2\text{p}3$, $\text{In}3\text{d}$ photoelectron spectra measured for different depth of TIC before and after freezing, which is tested by XPS. c) Tensile stress versus strain for TICs with different droplets radius (12, 20, 50, and 140 μm) and elastic modulus versus different radius. d) Microscopy image of TIC with different liquid metal loadings ($\varphi = 10\%$, 30%, and 50%). TIC ($\varphi = 40\%$) fabricated with different stirring time (60, 120, 180, 240, and 300 s) and the longer the stirring time, the smaller the droplets size, the scale bar is 200 μm . e) SEM image of the bottom side of TIC with stirring time of 360 s.

high rigidity of the PVC after vitrification limited the expansion and interconnection of liquid metal after freezing.

In brief, both the volume variation of liquid metal due to phase change and stiffness change of silicone polymer vitrification according to the temperature change lead to the reversible metal-insulator transition. It should be pointed out that the trigger mechanism is also applicable to some polymers and liquid metal composites such as liquid metal-PDMS.

To quantitatively predict the expansion and deformations of liquid metal droplets induced by freezing, here we built up a simplified model to illustrate the relationship between droplets size and electrical connection. We assume that the liquid metal droplets are spherical and uniformly embedded in the nonconductive polymer shell (Figure S6, Supporting Information). The surface of liquid metal placed in the polymer is tightly covered by the layer of a nonconductive film. In order to achieve conduction, it is necessary for liquid metal to bulging out from the film. As we know, the volume V of sphere is $V = \frac{4}{3}\pi R^3$. The

average radius of LM droplets before freezing is R_0 while it is R after solidification. The ΔR of LM droplets after solidification can be estimated by

$$\Delta R = R_0 (\sqrt[3]{\alpha + 1} - 1) \quad (1)$$

where, the volumetric expansion ratio of gallium α during phase transition (solidify) is about 3.1%. Therefore, ΔR can be calculated by

$$\Delta R = 0.01R_0 \quad (2)$$

As mentioned above, the surface of liquid metal placed in the polymer is tightly covered by a shell of nonconductive polymer. In order to measure the thickness of silicone gel shell, we applied the X-ray photoelectron spectroscopy (XPS) to analyze the component of the bottom side of TIC with different depth (0, 110, 220, 330, 440, and 550 nm). The bottom surface (0 nm)

of TIC has the elements of C, O, Si and without gallium and indium (Figure 2b; Figure S7, Supporting Information), indicating the existence of silicone polymer. Gallium and indium elements appear together in the depth of 330 nm (Green line in Figure 2b), which represents the EGaIn. Therefore, the thickness of the shell is between 220 and 330 nm. What is more, the content of gallium and indium increases with the increasing depth. After freezing and warming, the TIC is subject to the same analysis by XPS. There is no gallium and indium on the surface of the bottom side of TIC too, indicating no liquid metal releases on the surface, which is consistent with the microstructure of TIC. Different from the TIC before freezing, gallium and indium elements emerge at the depth of 220 nm (blue line in lower of Figure 2b) rather than 330 nm. It means that the thickness of the silicone gel shell become thinner after freezing and warming. This result is a strong evidence for the aforementioned hypothesis that temperature change alters the interior structure of TIC.

The thickness of shell between two adjacent droplets is about 220 nm. In order to form the conductive circuit, the ΔR of two adjacent droplets expansion must be larger than the thickness d of polymer, which can be described by

$$2\Delta R > d \quad (3)$$

Theoretically, the R_0 should be larger than 11 μm thus two expanding droplets can be connected to be conductive. However, oversized droplets might cause the release of LM and the reduction of mechanical strength. Two TICs with LM size of $r = 140 \mu\text{m}$ and $r = 12 \mu\text{m}$ are pressed and only the TIC with larger size droplets is damaged accompanied by liquid metal release (Figure S8, Supporting Information). We have also performed experiments to elucidate the influence of LM size on the mechanical strength. Figure 2c presents stress-strain curves for TIC with four different droplet sizes ($r = 12, 20, 50$, and $140 \mu\text{m}$). From the data, the stiffness of TICs with different droplet sizes is studied by applying the elastic modulus in the regime of low strain (0–20% strain). The results show that as the sizes of LM droplets increase ($r = 12, 20, 50$, and $140 \mu\text{m}$), the elastic modulus decreases from 80 to 41.25 kPa (80, 71.25, 56.25, and 41.25 kPa respectively), which is consistent with the prediction. Therefore, the sizes of droplets should be well controlled by adjusting the stirring time. The longer stirring time, the smaller size of LM droplets.

It is found that only the bottom side other than the upper side of the TIC materials becomes conductive after deep freezing. As we know, the density of liquid metal (EGaIn) (6.3 g cm^{-3}) is larger than the silica gel (1.03 g cm^{-3}). So the liquid metal droplets are naturally settled to the bottom during the curing process, which would cause the sediment amount difference between the upper side and bottom side. From the 3D X-ray imaging by a computed tomographic (CT) scanner, it is evident that most of the liquid metal droplets are settled to the bottom side other than the upper part of TIC (Figure S9, Supporting Information). The longer curing time might cause the sufficient liquid metal settling as well as the thinner polymer shell on the bottom side, which is more likely to achieve connection of liquid metal and insulator–metal transition of TIC. On the contrast, when the curing time is too short

to deposit enough liquid metal, the bottom surface might not exhibit low-temperature conductivity characteristics. To support the hypothesis, freshly prepared liquid metal polymer composites are heated to accelerate the curing process. As predicted, the fabricated materials do not exhibit electrical conductivity at low temperature. The deposition amounts of liquid metal can be described as

$$\text{Amount} = \int \mu_t dt \quad (4)$$

In addition to the curing time (sedimentation time), the sedimentation velocity μ_t also influences the liquid metal sediment amounts. Several experiments are conducted to explore the relationship between velocity and insulator–metal transition. There are many factors that can influence the settling process of LM droplets during the curing process of the polymer. The settling velocity μ_t can be described as Stokes formula

$$\mu_t = \frac{d^2 (\rho_l - \rho)}{18\mu} \quad (5)$$

where, d is the diameter of the liquid metal droplet, ρ_l and ρ is the density of liquid metal and silicone respectively, and μ is the viscosity of the fluids.

From the Equation (5), there are four factors that influence the settling velocity, including droplets size, viscosity μ , and density of liquid metal and silicone matrix. Because the density of two materials is constant, the larger size of liquid metal droplets and the lower viscosity of silicone substrate would lead to the faster settling velocity.

The experimental results show that the viscosity of TIC increases with stirring time increasing. After stirring for 5 min, the liquid compounds almost solidified without the settling process of liquid metal, which is, predictably, nonconductive when subjected to deep freezing (lower than 212 K). Figure S10 in the Supporting Information shows the electrical transition behaviors of TIC (40 vol% LM) with different stirring time (60, 120, 180, 240, and 300 s). It is unable to be conductive after freezing for the TIC with the stirring time 180, 240, and 300 s. On the contrary, TIC with shorter stirring time (60 and 120 s) can present electrically conductive state after freezing. The microstructure of the bottom side of TIC with different stirring time (60, 180, and 300 s) is shown in Figure 2d, where the droplet size decreases with the stirring time increasing. From Equation (5), the smaller size leads to the slower settling velocity of liquid metal, which is consistent with the results. The longer stirring time leads to the smaller size of LM droplets as well as larger viscosity of freshly prepared composites, both of which decrease the settling velocity LM droplets according to the Stokes formula. According to the Equation (3), smaller size of LM droplets is difficult to connect and form a conductive path after freezing. Figure 2e shows scanning electron microscopy (SEM) image of TIC stirring for 360 s, where the diameter of droplets is very small (smaller than 5 μm) and cannot exhibit conductive property even with extremely low temperature. Therefore, the stirring time cannot be long. However, a short stirring time leads to uneven distribution of LM in TIC. Although droplets are uneven in TIC, the experimental results show that electrical transition can repeat many

times without the resistance degradation. These results can be explained as follows: polymer in TIC has good elasticity and can recover to its original shape after freezing and warming. After several cycles of freezing, the LM droplet is sealed in the polymer shell without release (Figure S1, Supporting Information). Therefore, although the contact area between uneven droplets is not robust like the uniform droplets, there is little influence on the capability of connection of LM droplets (conductive) in TIC according to the experimental data.

It is found that the liquid metal loading ratio in TIC affects the conductive properties. TICs with different volume proportion of liquid metal have been frozen by liquid nitrogen and there is no electrical transition after freezing when contains more than 70 vol% liquid metal. It is strange that the higher proportion of liquid metal, a conductive substance, in the compounds would lead to the nonconductive capability. There are two reasons that can explain the results. At first, metallurgical microscope image shows that the size of droplets is reduced with the increase of liquid metal proportion (10%, 30%, 50%, Figure 2d). As previously mentioned, the decreasing droplets size would result in a decrease of settling speed. Besides, compounds containing higher contents of liquid metal are likely to be more viscous after stirring for the same time. Materials with 70 vol% liquid metal are extremely viscous after stirring for 120 s and decrease the sedimentation rate of liquid metal, resulting in the deficient liquid metal droplets on the bottom side. From Equation (5), larger viscosity leads to the lower settling speed of LM droplets. Therefore, the larger ratio of liquid metal influences the temperature electrical transition from two aspects: increasing the viscosity and decreasing droplets size, both of which can decrease the settling speed, impeding the sediment deposition amounts of liquid metal droplets. TIC lacks the ability of electrical transition when the LM weight percentage is lower than 5% (stirring time: 180 s). However, the threshold is not only related to the weight ratio, but also influenced by droplets size, which is controlled by stirring time. Thus, the minimum weight percentage value may vary to some extent.

In order to further verify the effect of viscosity directly, we add a thickener into the polymer (viscosity 1000, curing for 30 min) to increase viscosity and then mixed them with the liquid metal (40 vol%, 120 s). As expected, the bottom surface of the material is nonconductive after freezing with liquid nitrogen.

The above experimental results fully demonstrate that the curing time (the natural deposition time), the viscosity of the silica gel, liquid metal proportion as well as stirring time do affect the insulator–metal transition by influencing the sediments of the LM droplets. Therefore, in order to successfully prepare the TIC, the proper and accurate fabrication methods should be taken seriously.

TIC owns super stretchability and is capable of being stretched up to 680% strain and load up to 500% strain for 1000 cycles (Figure S11, Supporting Information). Stretched TIC is also capable of transforming between insulator and conductor in response to the freezing and heating (Figure 3a), expanding its potential application in stretchable electronics and switches. Moreover, there is no significant increase in the resistance of TIC (freezing) with larger strain. Figure 3a shows the normalized resistance curves of TIC (freezing) with

different strains (500%, 400%, 300%, 200%, 100%, and 0%) and the resistance keeps relatively stable. According to the previous study, stretching of the liquid metal polymer does not significantly influence the resistance.^[38] As mentioned above, it is the liquid metal expands and breaks out of the silicone shell that forms the conductive path. After stretching, the thickness of the flexible outer shell might change, and the distance between the liquid metal droplets will also change. Why can liquid metal droplets also be contacted after freezing? Another model was built to explain this result (Figure S12, Supporting Information). When TIC is stretched, the microscale liquid metal droplets would deform into spindle shapes and the distances along the stretching direction/longitudinal direction would increase (Figure S13, Supporting Information). As EGaIn based liquid metal is an isotropic material, it will bulge uniformly after freezing thus the size change along the longitudinal direction will be larger than the radial direction and diminish the impact of distance increase.

As we know, response time and current stability are crucial for potential applications such as switches, sensors or resistive random access memory. As shown in Figure 3b, the current changes in response to freezing and warming are recorded. A constant voltage ($U = 3$ V) and a series resistor ($R = 3.6 \Omega$) are applied for protecting the circuit. We start to freeze TIC at 64 s and current increases at about 66 s. At 70 s, the currents reach the peak and keep constant until TIC is warmed at 380 s. The current drops 83.7% in 6 sec and reaches zero in the next 2 sec. Therefore, the transition from the insulator (Current = 0 A) to conductor needs only 2 sec and the reverse process (from conductor to insulator) needs about 8 sec. Figure 3b,c demonstrates several cycles of increase and decrease of current as freezing and warming. The maximum current remains constant after several temperature change cycles. Based on the above electrical properties, we developed an intelligent switch for the electrical circuit in a minicar that only depends on temperature regulation.

We conduct experiments about a temperature-controlled movement of minicar applied with the TIC ($\varphi = 40\%$). The insulative TIC is inserted and supersedes a part of the electric circuit in the minicar, serving as a variable resistance and controlling the circuits status between connection and disconnection (Figure 3d). Frozen by the liquid nitrogen, the TIC becomes electrically conductive and connects the circuit, driving the minicar immediately. With the temperature rise, resistance increases and the power of minicar damps, reducing the speed until it stops. (Figure 3e; Movie S4, Supporting Information). It would move when subjected to freezing again. From Figure 3b, the current keeps constant at the freezing status. It is expected that minicar would move in low temperature until the battery was used up.

Because the TIC changes its electric state (on/off ratio is 10^9) only according to the temperature, rendering it a transducer that converts the temperature into different resistance and binary signal ("0," "1"), it can be applied as a stretchable temperature sensor or resistive random access memory. Starting from this point, we conceived a temperature dependent digital display system that can display different numbers and letters on a computer in response to the temperature change of TIC. The display system is composed of the single-chip microcomputer with sixteen TIC as sensors, a Bluetooth module, and user

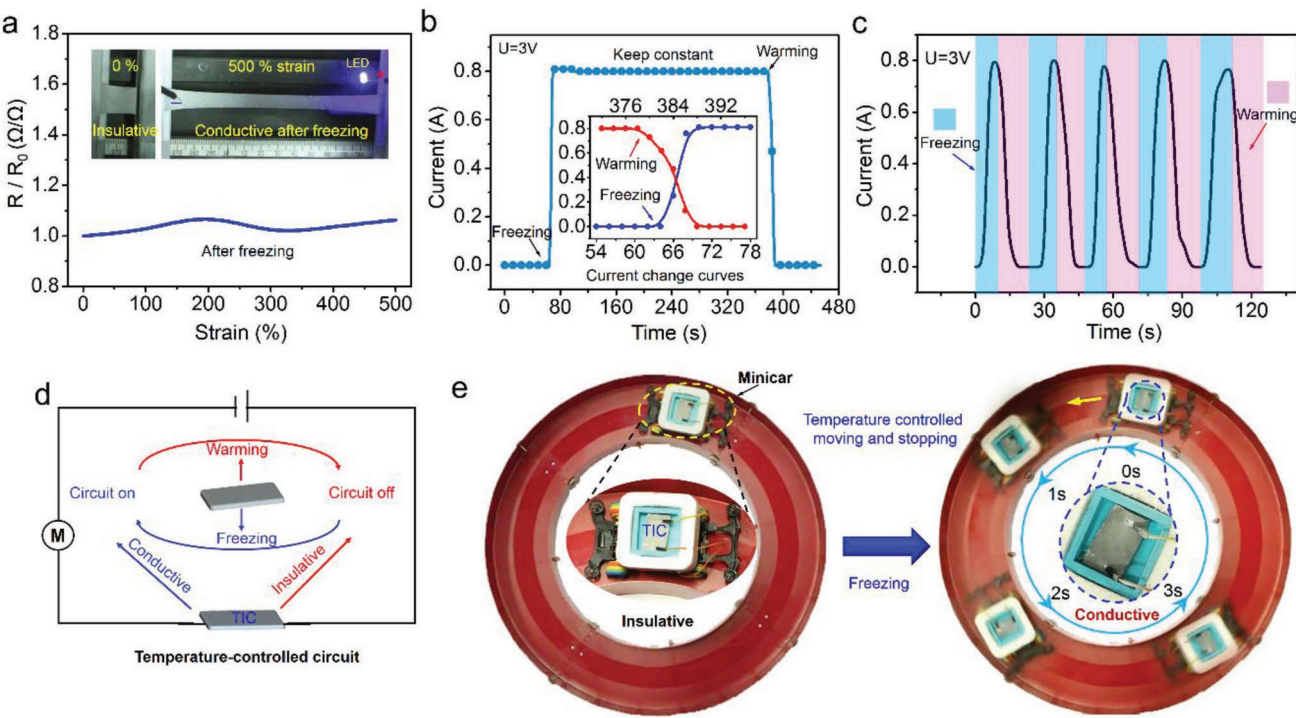


Figure 3. Temperature-controlled stretchable switches for turning on or off automatically based on TIC ($\varphi = 40\%$). a) Normalized resistance after freezing as a function of strain and TIC maintains the properties of transition between insulator and conductor reversibly after stretching. b) Current change after following steps: freezing from 64 to 380 s and then warming, which applied a constant voltage ($U = 3 \text{ V}$) and a series resistor ($R = 3.6 \Omega$) for protecting the circuit. c) Current change curves after undergoing several freezing–warming cycles, where the blue areas represent freezing with liquid nitrogen while the purple areas represent warming with hot water (333 K). d) Circuit schematic diagram of a soft temperature switch based on the TIC. e) The insulative TIC is inserted and supersedes a part of an electric circuit in the minicar, which serves as a soft temperature switch in the circuit diagram. When freezing, TIC becomes conductive and the minicar starts to move, which stops when the temperature of TIC rises.

interface of the software (Figure 4a; Figure S13a, Supporting Information). There are freezing liquid and warming liquid that supply different temperature environments (“low” “high”) of TIC as required. TIC with infinite resistance ($R > 1 \text{ M}\Omega$) when putting in warming liquid would convert to “0” through A/D converters in the microcomputer and wireless Bluetooth module (Figure 4b; Figure S13b, Supporting Information). In the same way, the system would convert the resistance of TIC in freezing liquid into “1.” Here, “0” and “1” can be presented with different color squares (green represents 1, purple represents 0) on the user interface of the software (Figure S13c, Supporting Information). Figure 4c shows the “T,” “H,” and “U” on the user interface of the software with a 3 by 3 pixel array, which represents the abbreviation of Tsinghua University. The color of pixels could change according to the on/off states of TICs, e.g., the freezing/warming state of every single TIC, thus the software display depends on temperature variations. For example, in order to display “T” with different colors of nine squares, nine A/D converters are dipping into different liquids. Specifically, the color changes of the square with label “1” in Figure 4c result from dipping into freezing liquids of TIC. Therefore, continually regulating the temperature of each TIC is able to display different letters or other characters. Figure 4d shows the single-chip microcomputer with 15 TIC A/D converters and the user interface of the software with a 5 by 3 pixel array, which can display different numbers via

temperature regulation of each TIC (Movie S5, Supporting Information). The source code of the developed software is provided in the experimental section.

Therefore, TIC offers a promising possibility to be served as a stretchable phase change memory, which has attracted much attention in the scientific and industrial field.^[39,40] With the low-temperature induced electrical transition, TIC can also serve as a low-temperature alarm system. Although the temperature threshold (212 K) to trigger the conductivity of TIC is too low and limit its wide application in some extent, the ultralow temperature environment in outer space may provide excellent application environments such as the electrical switch in response to deep temperature stimulus. As we know, the average surface temperature of Mars is 210 K; the average temperature in the inland plateau of Antarctica is about 221 K, the extreme minimum temperature has reached 183.8 K; the temperature on the moon can reach 399 K, and the average temperature at night can be as low as 93 K. All of the above environments are faced with the problem of low-temperature failure of electronic devices, and the circuit control is more difficult due to the uninhabited situation. The critical transition temperature of the TIC is about 212 K. When the temperature is lower than the threshold (212 K), it shows conductivity. When the temperature becomes higher than the threshold, it depicts insulation, which can achieve perfect matching with the above-mentioned low-temperature environments. It can therefore

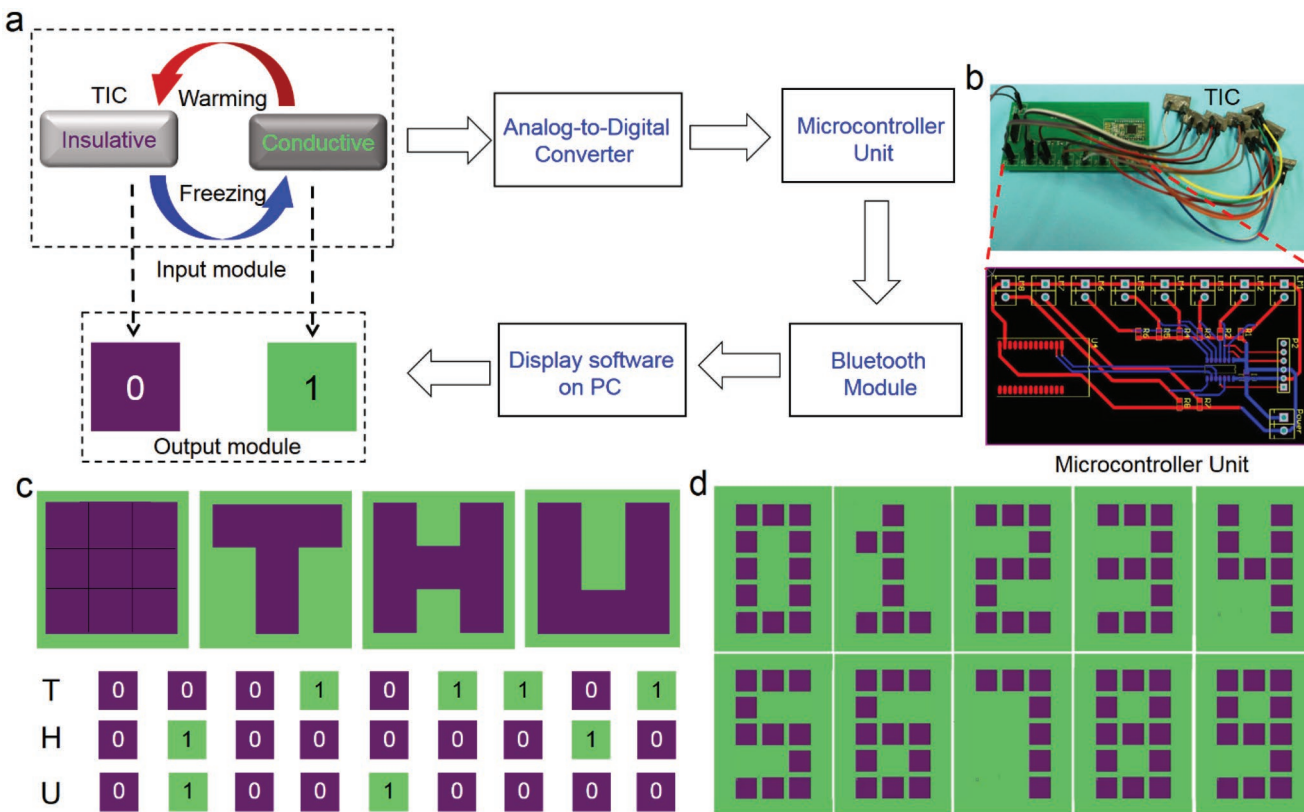


Figure 4. Temperature-controlled digital display based on the reversible electrical transition of TIC. a) Schematic diagram of the temperature controlled digital display. The conductive/insulative states transition of TIC can be converted into the binary state: 1 or 0, which is displayed with green and purple squares respectively. b) The TIC is inserted in the input module and connect with the microcontroller unit, which can change electrical state in response to temperature regulation. c) Here is an example of TIC display with a 3 by 3 pixel array, nine TIC are implemented to regulate the display. 1 represents low temperature while 0 represents the high temperature of TIC. Three characters of "T," "H," and "U" are shown, which is the abbreviation of Tsinghua University. d) With a 5 by 3 pixel array, all ten numbers visualization could be achieved by dipping TIC into liquid nitrogen or hot water.

be applied to the following situations, for example, the temperature drops suddenly at night on Mars or the Moon, which makes this material change from the insulator to conductor spontaneously, and then the circuit is automatically turned on. When the night falls, the circuit starts lighting based on the properties of such material. When the day time is coming, the circuit is disconnected as the temperature rises. This device not only saves energy but also reduces the investment required to control the systems. TIC would play an important role in the future exploration of outer space and polar scientific research, indicating great application prospects.

The transition between the conductivity and insulation of the materials designed herein can be used in phase change memories to store information. When solidified, the material is electrically conductive and can be used to write information. When melted, the material becomes insulating and can be used to erase information. At the same time, because of the difference of 31 K, the writing process and the erasing process of the phase change memory are performed in different temperature intervals, which significantly improve the accuracy and practicability of the phase change memory. Besides, this material can also be used for cold energy storage, which would be solidified at a low temperature (212 K) to store cold energy and then melted at a higher temperature (243 K) to

release it. Here, the existence of temperature difference can drive the material to solidify rapidly and improve the efficiency of cold storage. Although the temperature threshold is too low to be used for normal switches conveniently. At this stage, our study is mainly focused on disclosing the general mechanism and presenting a novel method (temperature regulation) to achieve electrical transition reversibly in liquid metal polymer composites, which might inspire future study about low temperature electronics and facilitate the exploration of the polar region.

To summarize, a highly stretchable (680% strain) liquid metal polymer with the capability of a temperature-controlled reversible electrical transition between insulator and conductor was demonstrated. The liquid metal droplets are enclosed with the insulative silicone shell and it is nonconductive. Under low temperature condition ($T = 212$ K), the liquid metal droplets solidify and expand in volume, whereas the insulating polymer shrinks and becomes rigid, leading to the connection of liquid metal (conductive). It would recover to the initial state when heating. Furthermore, a simplified model has been built up to quantitatively predict the expansion and connection of liquid metal droplets. The electrical transition cycles between insulator and conductors have been demonstrated for more than 100 times without structural damage. Importantly, only with the

proper fabrication methods, such as appropriate liquid metal loading content, stirring time, curing time, TIC can achieve insulator–metal transition by freezing or heating, which is fully clarified in this study. TIC has the ability to easily (just freezing and heating), rapidly (3 sec), dramatically (10^9 times) and reversibly (100 times without degradation) change resistivity as necessary, which presents tremendous application potential in wide areas. Lower electrical transition temperature (about 212 K) limits some applications on earth. However, Antarctica and outer space planets such as Mars may provide a superexcellent application environment for such material. Lastly, this study reveals a universal strategy to achieve the reversible insulator–metal transition materials, whose working mechanism would help incubate diverse and unconventional liquid hybrid materials.

Experimental Section

Preparation of TIC: The fabrication method of this material was straightforward and fast. Different proportions of liquid metal (75.5% gallium, 24.5% indium) were thoroughly mixed with polymer (methyl vinyl polysiloxane and Pt-catalyzed polymethylhydrosiloxane mixed at 1:1 volume ratio) and then cured for a proper time, which depends on the liquid metal loading content. Mechanical stirring time and curing time was important to fabricate the TIC. The 40 vol% LM loading was selected, stirred for 2 min at the speed of 600 rpm to fabricate the TIC that was applied in the study excepted where noted. The PDMS and ecoflex-0030 were also chosen as polymer matrix for the contrast test.

Freezing and Heating Methods: Considering the convenience and better freezing effect, the liquid nitrogen (boiling point 77 K) was applied to freeze the TIC. Cryogenic refrigerator was also chosen as freezing methods in some experiments. Warming process was achieved by hot water (about 333 K) or heating gun depends on the requirement.

Electrical Properties Testing: Lower resistance was tested based on Ohm's law $R = \frac{U}{I}$. A constant voltage ($U = 3$ V) and a series resistor ($R = 3.6 \Omega$) for protecting the circuit was applied. Larger resistance was tested by multimeter, which could test the resistance up to $200 \text{ M}\Omega$. Current was measured directly with Agilent. The resistivity of TIC as a function of temperature was measured by PPMS.

Materials Characterization: The element composition of TIC was tested by XPS (PHI Quanta II). Microstructure photos of TIC were obtained from the metallographic microscope and SEM S4800. Storage modulus and loss modulus as well as glass transition temperature were tested by Dynamic Thermomechanical Analysis Q800. 3D structure of TIC was obtained by a CT scanner (Carl Zeiss Xradia 410 versa).

Display System Implementation: Source code

```
Import processing.serial.*;
Serial myPort;
byte[] buffer = new byte[10];
byte[] inputValue = new byte[8];
void setup()
{
    myPort = new Serial(this,"COM3",9600);
    size(650,650);
    strokeWeight(30);
    background(255);
}
void draw()
{
    println("ttt");
    if(myPort.available()>0)
    {
        println("yyy");
    }
}
```

```
String end = "CCCC";
byte flag[] = end.getBytes();
int flag = -52;
val = myPort.readStringUntil('\n');
myPort.readBytesUntil(flag,buffer);
buffer = myPort.readBytes();
if (buffer != null){
    println("xxx");
    String myString = new String(buffer);
    println(buffer);
}
background(100,200,100);
noStroke();
fill(100,buffer[9]*200,100);
rect(450,450,150,150);
fill(100,buffer[2]*200,100);
rect(250,50,150,150);
fill(100,buffer[3]*200,100);
rect(450,50,150,150);
fill(100,buffer[4]*200,100);
rect(50,250,150,150);
fill(100,buffer[5]*200,100);
rect(250,250,150,150);
fill(100,buffer[6]*200,100);
rect(450,250,150,150);
fill(100,buffer[7]*200,100);
rect(50,450,150,150);
fill(100,buffer[8]*200,100);
rect(250,450,150,150);
fill(100,0,100);
rect(50,50,150,150);
}
```

Supporting Information

Supporting Information is available from the Wiley Online Library or from the author.

Acknowledgements

H.W. and Y.Y. contributed equally to this work. The authors thank for the help of Weiwei Wu, Rui Guo, Hongpeng Li, Xiaoqi Wang, and Linlin Fan (Tsinghua University) in the materials characterization. This work was partially supported by National Nature Science Foundation of China under Key Project # 91748206, Dean's Research Funding of the Chinese Academy of Sciences, and the Frontier Project of the Chinese Academy of Sciences. All authors declared that there were no competing financial interests.

Conflict of Interest

The authors declare no conflict of interest.

Keywords

liquid metals, phase change, reversible transitional insulator and conductor, soft and stretchable electronics

Received: February 27, 2019
Published online: April 11, 2019

- [1] M. M. Qazilbash, M. Brehm, B.-G. Chae, P.-C. Ho, G. O. Andreev, B.-J. Kim, S. J. Yun, A. Balatsky, M. Maple, F. Keilmann, *Science* **2007**, *318*, 1750.
- [2] R. Moore, J. Zhang, V. B. Nascimento, R. Jin, J. Guo, G. Wang, Z. Fang, D. Mandrus, E. W. Plummer, *Science* **2007**, *318*, 615.
- [3] S. R. Ovshinsky, *Phys. Rev. Lett.* **1968**, *21*, 1450.
- [4] N. Ogihara, N. Ohba, Y. Kishida, *Sci. Adv.* **2017**, *3*, e1603103.
- [5] A. A. Talin, A. Centrone, A. C. Ford, M. E. Foster, V. Stavila, P. Haney, R. A. Kinney, V. Szalai, F. El Gabaly, H. P. Yoon, *Science* **2014**, *343*, 66.
- [6] T. Chen, K. Reich, N. J. Kramer, H. Fu, U. R. Kortshagen, B. Shklovskii, *Nat. Mater.* **2016**, *15*, 299.
- [7] J. C. Hill, A. T. Landers, J. A. Switzer, *Nat. Mater.* **2015**, *14*, 1150.
- [8] H. Akinaga, H. Shima, *Proc. IEEE* **2010**, *98*, 2237.
- [9] E. J. Yoo, M. Lyu, J. H. Yun, C. J. Kang, Y. J. Choi, L. Wang, *Adv. Mater.* **2015**, *27*, 6170.
- [10] F. Morin, *Phys. Rev. Lett.* **1959**, *3*, 34.
- [11] T. Hickmott, *J. Appl. Phys.* **1962**, *33*, 2669.
- [12] C. Wu, H. Wei, B. Ning, Y. Xie, *Adv. Mater.* **2010**, *22*, 1972.
- [13] K. Szot, W. Speier, G. Bihlmayer, R. Waser, *Nat. Mater.* **2006**, *5*, 312.
- [14] Z. Liao, N. Gauquelin, R. J. Green, K. Müller-Caspary, I. Lobato, L. Li, S. Van Aert, J. Verbeeck, M. Huijben, M. N. Grisolia, *Proc. Natl. Acad. Sci. USA* **2018**, *115*, 9515.
- [15] J. C. Scott, L. D. Bozano, *Adv. Mater.* **2007**, *19*, 1452.
- [16] R. E. Holmlin, R. Haag, M. L. Chabinyc, R. F. Ismagilov, A. E. Cohen, A. Terfort, M. A. Rampi, G. M. Whitesides, *J. Am. Chem. Soc.* **2001**, *123*, 5075.
- [17] J. Park, I. You, S. Shin, U. Jeong, *ChemPhysChem* **2015**, *16*, 1155.
- [18] S. Wang, J. Xu, W. Wang, G.-J. N. Wang, R. Rastak, F. Molina-Lopez, J. W. Chung, S. Niu, V. R. Feig, J. Lopez, *Nature* **2018**, *555*, 83.
- [19] J. Hughes, F. Iida, *Sensors* **2018**, *18*, 3822.
- [20] R. E. Rivero, M. A. Molina, C. R. Rivarola, C. A. Barbero, *Sens. Actuators, B* **2014**, *190*, 270.
- [21] B. Xu, D. Chen, R. C. Hayward, *Adv. Mater.* **2014**, *26*, 4381.
- [22] S. Stassi, G. Canavese, *J. Polym. Sci., Part B: Polym. Phys.* **2012**, *50*, 984.
- [23] G. Lee, T. Lee, Y. W. Choi, P. V. Pikhitsa, S. J. Park, S. M. Kim, D. Kang, M. Choi, *J. Mater. Chem. C* **2017**, *5*, 10920.
- [24] P. Meng, Q. Zhang, Y. Wu, Z. Tan, G. Cheng, X. Wu, R. Zheng, *Adv. Funct. Mater.* **2017**, *27*, 1701136.
- [25] P. Sun, Y. Wu, J. Gao, G. Cheng, G. Chen, R. Zheng, *Adv. Mater.* **2013**, *25*, 4938.
- [26] G. Liu, X. Zhuang, Y. Chen, B. Zhang, J. Zhu, C.-X. Zhu, K.-G. Neoh, E.-T. Kang, *Appl. Phys. Lett.* **2009**, *95*, 327.
- [27] L. Sheng, J. Zhang, J. Liu, *Adv. Mater.* **2014**, *26*, 6036.
- [28] S. Mei, Y. Gao, Z. Deng, J. Liu, *J. Electron. Packag.* **2014**, *136*, 011009.
- [29] M. D. Dickey, *Adv. Mater.* **2017**, *29*, 1606425.
- [30] Z. Yu, J. Shang, X. Niu, Y. Liu, G. Liu, P. Dhanapal, Y. Zheng, H. Yang, Y. Wu, Y. Zhou, *Adv. Electron. Mater.* **2018**, *4*, 1800137.
- [31] K. Chu, B. G. Song, H. I. Yang, D. M. Kim, C. S. Lee, M. Park, C. M. Chung, *Adv. Funct. Mater.* **2018**, *28*, 1800110.
- [32] E. J. Markvicka, M. D. Bartlett, X. Huang, C. Majidi, *Nat. Mater.* **2018**, *17*, 618.
- [33] A. Fassler, C. Majidi, *Adv. Mater.* **2015**, *27*, 1928.
- [34] M. D. Bartlett, A. Fassler, N. Kazem, E. J. Markvicka, P. Mandal, C. Majidi, *Adv. Mater.* **2016**, *28*, 3726.
- [35] N. Kazem, M. D. Bartlett, C. Majidi, *Adv. Mater.* **2018**, *30*, 1706594.
- [36] B. E. Schubert, D. Floreano, *RSC Adv.* **2013**, *3*, 24671.
- [37] L. Ren, J. Zhuang, G. Casillas, H. Feng, Y. Liu, X. Xu, Y. Liu, J. Chen, Y. Du, L. Jiang, *Adv. Funct. Mater.* **2016**, *26*, 8111.
- [38] C. Majidi, *Robotic Systems and Autonomous Platforms*, Woodhead Publishing, Cambridge, UK **2019**, pp. 425–448.
- [39] X. Zhou, J. Kalikka, X. Ji, L. Wu, Z. Song, R. E. Simpson, *Adv. Mater.* **2016**, *28*, 3007.
- [40] M. Salinga, B. Kersting, I. Ronneberger, V. P. Jonnalagadda, X. T. Vu, M. Le Gallo, I. Giannopoulos, O. Cojocaru-Mirédin, R. Mazzarello, A. Sebastian, *Nat. Mater.* **2018**, *17*, 681.